The effect of zonally asymmetric ozone heating on the Northern Hemisphere winter polar stratosphere

J. P. McCormack[1], T. R. Nathan[2], E. C. Cordero[3]

J. P. McCormack, Naval Reseach Laboratory, Washington DC, 20375, USA.

T. R. Nathan, Atmospheric Science Program, Department of Land, Air and Water Resources University of California, Davis, CA, 95616, USA.

E. C. Cordero, Department of Meteorology and Climate Science, San Jose State University, San Jose, CA 95192, USA.

[1]Space Science Division, Naval Research Laboratory, Washington DC, USA.

[2]Department of Air, Land, and Water Resources, University of California, Davis CA, USA.

[3]Department of Meteorology and Climate Science, San Jose State University, San Jose CA, USA.

Report Documentation Page

Form Approved
OMB No. 0704-0188

1. REPORT DATE	2. REPORT TYPE	3. DATES COVERED
09 DEC 2010		**00-00-2010 to 00-00-2010**

4. TITLE AND SUBTITLE	5a. CONTRACT NUMBER
The effect of zonally asymmetric ozone heating on the Northern Hemisphere winter polar stratosphere	5b. GRANT NUMBER
	5c. PROGRAM ELEMENT NUMBER
6. AUTHOR(S)	5d. PROJECT NUMBER
	5e. TASK NUMBER
	5f. WORK UNIT NUMBER
7. PERFORMING ORGANIZATION NAME(S) AND ADDRESS(ES) **Naval Reseach Laboratory,Space Science Division,Washington,Dc,20375**	8. PERFORMING ORGANIZATION REPORT NUMBER
9. SPONSORING/MONITORING AGENCY NAME(S) AND ADDRESS(ES)	10. SPONSOR/MONITOR'S ACRONYM(S)
	11. SPONSOR/MONITOR'S REPORT NUMBER(S)

12. DISTRIBUTION/AVAILABILITY STATEMENT
Approved for public release; distribution unlimited

13. SUPPLEMENTARY NOTES

14. ABSTRACT

15. SUBJECT TERMS

16. SECURITY CLASSIFICATION OF:			17. LIMITATION OF ABSTRACT	18. NUMBER OF PAGES	19a. NAME OF RESPONSIBLE PERSON
a. REPORT **unclassified**	b. ABSTRACT **unclassified**	c. THIS PAGE **unclassified**	**Same as Report (SAR)**	**16**	

Previous modeling studies have found significant differences in winter extratropical stratospheric temperatures depending on the presence or absence of zonally asymmetric ozone heating (ZAOH), yet the physical mechanism causing these differences has not been fully explained. The present study describes the effect of ZAOH on the dynamics of the Northern Hemisphere extratropical stratosphere using an ensemble of free-running atmospheric general circulation model simulations over the 1 December - 31 March period. We find that the simulations including ZAOH produce a significantly warmer and weaker stratospheric polar vortex in mid-February due to more frequent major stratospheric sudden warmings compared to the simulations using only zonal mean ozone heating. This is due to regions of enhanced Eliassen-Palm flux convergence found in the region between 40°N–70°N latitude and 10–0.05 hPa. These results are consistent with changes in the propagation of planetary waves in the presence of ZAOH predicted by an ozone-modified refractive index.

1. Introduction

Current climate change assessments have examined atmosphere-ocean general circulation model (GCM) simulations that include the effects of stratospheric ozone depletion in addition to increasing greenhouse gas emissions [e.g., Meehl et al., 2007]. Because of limited computational resources, these long-term simulations typically use a prescribed zonal mean ozone climatology to compute stratospheric heating rates [Cordero and Forster, 2007]. A number of recent studies have suggested that using prescribed zonally symmetric ozone heating, thereby neglecting zonally asymmetric ozone heating (ZOAH) effects, may affect the accuracy of the simulations by failing to capture important radiative-dynamical feedbacks involving ozone heating and planetary wave propagation [Perlwitz et al., 2008; Son et al., 2008; Waugh et al., 2009]. Modeling studies by, e.g., Gabriel et al. [2007]; Crook et al. [2008]; Waugh et al. [2009]; Gillett et al. [2009] have investigated these feedbacks and found that ZAOH tends to produce a colder (warmer) winter polar stratosphere in the Southern (Northern) hemisphere. However, the exact physical mechanisms through which ZAOH affects the polar winter stratosphere has not yet been fully explained.

An important first step in identifying the mechanisms that may connect ZAOH with the polar winter stratosphere has been provided by Nathan and Cordero [2007], who present a theoretical framework for understanding how ZAOH operates on the zonal-mean circulation. Their theory, based on quasigeostrophic formalism, hinges on an ozone-modified refractive index (OMRI) that explicitly shows how ZAOH modifies the vertical propagation and damping of planetary Rossby waves. Together, these ozone-modified wave properties modulate the Eliassen-Palm

flux divergence, a fundamental measure of the planetary wave drag on the zonal-mean circulation.

The goal of the present study is to expand on the one-dimensional (in height) quasigeostrophic results of Nathan and Cordero [2007] by examining the effects of ZAOH on the dynamics of the Northern Hemisphere (NH) winter polar stratosphere using a high-altitude version of the Navy Global Atmospheric Prediction System (NOGAPS) GCM, designated NOGAPS-ALPHA (Advanced Level Physics-High Altitude). This study focuses on the period from 1 December to 31 March, since planetary wave activity is much stronger in NH winter than in Southern Hemisphere (SH) winter. In general, our results agree with earlier studies showing that ZAOH produces a warmer winter polar stratosphere than zonally symmetric ozone heating. We present the first evidence that ZAOH acts to increase the chances for a stratospheric sudden warming (SSW) to occur, which is consistent with the changes in planetary wave propagation and damping during NH winter predicted by the OMRI of Nathan and Cordero [2007]. These results may help to understand observed correlations between decadal variations in solar ultraviolet irradiance, stratospheric ozone, and planetary wave activity that have often been cited as possible mechanisms linking solar activity to climate.

2. Model Description and Methodology

The GCM component of NOGAPS-ALPHA used in the present study is a global spectral model using a triangular truncation at wave number 79 and 68 hybrid (σ-p) vertical levels extending from the surface to 5×10^{-5} hPa ($\sim$90 km). The effective horizontal grid spacing is 1.5° in latitude/longitude and the effective vertical grid spacing is $\sim$ 2 km in the stratosphere. Shortwave heating and longwave cooling rates are computed using prognostic O_3 and H_2O

fields and a fixed vertical profile of CO_2. Photochemical sources and sinks of both O_3 and H_2O are specified using the parameterizations of McCormack et al. [2006]; McCormack et al. [2008], respectively. The model is forced at the lower boundary using observed 12-hourly sea surface temperature and surface ice distributions. For a more detailed description of the NOGAPS-ALPHA forecast model, see Eckermann et al. [2009] and McCormack et al. [2009], and references therein.

To investigate the effects of ZAOH on the dynamics of the NH winter polar stratosphere, two sets of free-running NOGAPS-ALPHA model simulations were performed. Each set is initialized identically using analyzed wind, temperature, and constituent fields from the high-altitude NOGAPS-ALPHA data assimilation system [Hoppel et al., 2008; Eckermann et al., 2009]. Each simulation is 120 days in length, beginning in early December and extending to the end of March, with output every 12 hours. The first set of model simulations (designated 3DO3) uses the full 3D prognostic ozone field in the radiative heating and cooling calculations. The second set (designated ZMO3) uses the zonal mean value of the prognostic ozone in the radiative heating and cooling calculations at each longitude grid point for that particular latitude, thus neglecting the ZAOH component. By taking the difference between the 3DO3 and ZMO3 results, one can isolate the effects of the ZAOH component. This approach differs from earlier studies by Gabriel et al. [2007] and Crook et al. [2008], which imposed zonal asymmetries in the modeled ozone heating rates rather than using self-consistent 3D ozone fields calculated from the model transport. We note that the zonal mean ozone values are nearly identical between the individual pairs of 3DO3 and ZMO3 runs throughout most of the time period. Only at high latitudes in February and March below the height of the 10 hPa level ($\sim$30 km) do small ($<$10%)

differences emerge, when the model dynamics eventually diverge enough to impact the zonal mean ozone distribution.

To assess the statistical significance of the ZAOH effects, an ensemble of NOGAPS-ALPHA simulations was generated, consisting of 15 pairs of 3DO3 and ZMO3 simulations. Each pair is initialized using the same set of initial conditions. For example, the first three pairs are initialized using the NOGAPS-ALPHA analyses for 00UT 1 December, 5 December, and 9 December 2007. The next three pairs are initialized using the model output fields at hour 12 from the first three simulations, and the following three pairs are initialized using the hour 24 output of the original three simulations, etc.

Comparison of zonal asymmetries in monthly mean ozone and temperature fields from the 3DO3 ensemble at 60°N and 10 hPa with observations from the NOGAPS-ALPHA assimilation for December 2007 – February 2008 (not shown) shows good overall agreement. This lends confidence in our ability to accurately describe the effects of ZAOH on the polar winter stratosphere.

3. Results

Figure 1a compares the time evolution of the ensemble mean 3DO3 (red curve) and ZMO3 (blue curve) model temperatures at 10 hPa averaged over 75°N-90°N latitude. For the first two weeks of the simulations, the 3DO3 and ZMO3 ensemble means are indistinguishable from each other. Throughout most of January and early February the 3DO3 ensemble mean is ∼5-6 K warmer than the ZMO3 ensemble mean. In mid-February this difference grows to 12 K. To illustrate the ensemble spread in the modeled 10 hPa polar temperatures, values of the 3DO3 ensemble average plus/minus its standard deviation are plotted in Fig. 1a as gray curves. A

Student's T-test is performed to assess the significance of the differences between the ensemble means at each time step. We find statistically significant temperature differences at the 95% confidence level over the Northern polar cap at 10 hPa on days 71-80, when the largest differences between the 3DO3 and ZMO3 ensembles occur.

Figure 1b plots the time evolution of the ensemble zonal mean zonal winds at 10 hPa between 50°N-60°N latitude in a manner similar to Fig. 1a (positive values denote westerly winds). Differences in the ensemble mean winds are negligible throughout much of December. In January, the 3DO3 mean westerly winds are $\sim$5 m s^{-1} weaker compared to the ZMO3 winds. By mid-February, the 3DO3 mean westerly winds are 10–14 m s^{-1} weaker than the ZMO3 case, concurrent with the largest temperature differences in Fig. 1a.

Figures 2 and 3 plot the latitude and altitude dependences of the monthly zonal mean temperature and zonal wind differences (3DO3-ZMO3) for December, January, February, and March, respectively. The temperature response in December (Fig. 2a) is negligible, while in January (Fig. 2b) there is evidence of a warming (cooling) in the midlatitude upper stratosphere (lower mesosphere) of $\sim$2 K. The largest temperature response is found in February, with a statistically significant warming in excess of 8 K in the polar stratosphere near 10 hPa. We also note a significant warming (cooling) in the equatorial (polar) mesosphere during this time. By March (Fig. 2d) the polar stratospheric warming is much weaker and limited to the region near 100 hPa, while the upper polar stratosphere exhibits cooling of $\sim$4 K, although neither of these features are statistically significant.

The zonal wind response in December (Fig. 3a) consists of a weak (2–3 m s^{-1}) easterly (westerly) anomaly in the lower (upper) equatorial mesosphere. The locations of these negative

(positive) zonal wind anomalies in December coincide with an equatorward (poleward) shift in the location of the zero wind line (not shown). In January (Fig. 3b), more pronounced easterly anomalies exceeding 10 m s^{-1} appear near the equatorial stratopause and in the extratropical upper stratosphere/lower mesosphere. By February (Fig. 3c), the extratropical easterly anomaly has propagated poleward and downward, similar to the positive temperature anomaly in Fig. 2.

In general, the temperature and zonal wind responses in Figs. 2 and 3 present a consistent picture of a warmer polar stratosphere and weaker polar vortex during January and February in the presence of ZAOH. The polar stratospheric warming/mesospheric cooling signature in Fig. 2c is characteristic of a SSW. An examination of the wind fields from the 30 individual ensemble members found 5 winters when a major SSW occurred during January or February. (Here we define a major SSW as a reversal of the zonal mean zonal wind at 10 hPa and 60°N from westerly to easterly flow.) Of these five cases, four took place in 3DO3 simulations (i.e., where ZAOH is included) and one took place in a ZMO3 simulation. Days with zonal mean easterly flow at 10 hPa and 60°N from the 3DO3 and ZMO3 ensembles are indicated by the red and blue horizontal lines, respectively, in Fig. 1b.

To better understand the origin of the temperature and zonal wind differences due to the effects of ZAOH that first emerge in January (Fig. 1), we examine how the modeled planetary wave activity affects the zonal mean zonal winds through differences in the Eliassen-Palm (EP) flux divergence between the 3DO3 and ZMO3 cases. Figure 4a plots the 3DO3 ensemble monthly mean EP-flux divergence over the Northern Hemisphere for January. Negative values, denoting convergence or an easterly acceleration, are present throughout much of the extratropical upper stratosphere and mesosphere. The ZMO3 EP-flux divergence for January (Fig. 4b)

shows generally smaller negative values of the EP flux divergence in the extratropical stratosphere, particularly between 60°N–70°N near 1 hPa. Figure 4c plots the difference between the EP flux divergence fields in Figs. 4a and 4b. Overall, we find greater planetary wave drag on the zonal mean flow in January in the presence of ZAOH. These results are consistent with the temperature and zonal wind responses described above. Specifically, stronger (weaker) EP flux convergence is associated with warmer (colder) polar stratospheric temperatures and a weaker (stronger) polar vortex in the presence (absence) of ZAOH.

4. Summary and Discussion

An ensemble of free-running GCM simulations has been used to isolate the effects of ZAOH on the temperature and wind distributions in the Northern winter stratosphere. We find that ZAOH produces a warmer and weaker polar vortex during January and February, and a higher frequency of major SSWs in mid-to-late February.

Although direct comparisons between the NOGAPS-ALPHA model results presented here and the quasigeostrophic model results of Nathan and Cordero [2007] are difficult, both models show that ZAOH produces significant changes in the EP-flux divergence and thus the zonal-mean zonal wind. In the extratropics, both models show that these ZAOH-induced changes extend from near ∼10 hPa (∼30 km) where wave-ozone advection and ozone photochemistry both contribute to the ZAOH effect, up to ∼0.01 hPa (∼65 km) where the ZAOH effect is controlled by ozone photochemistry. Overall, the present study indicates that in the absence of ZAOH, imposing only zonally symmetric ozone heating in a GCM will likely produce a colder, stronger NH winter polar vortex and fewer SSWs.

The temperature differences in Fig. 1a are generally similar to earlier results from Gillett et al. [2009] in that we find warmer winter polar stratospheric temperatures when ZAOH is included. However, Gillett et al. [2009] reported a maximum warming of approximately 3 K at 10 hPa in December only, with no statistically significant warming in January or February. While the exact reasons for this discrepancy are unknown at this time, we note that the higher frequency of major SSWs in the 3DO3 ensemble is primarily responsible for the statistically significant temperature and wind responses reported here. Many middle atmosphere GCMs tend to underpredict the occurrence of SSWs [Charlton et al., 2007]. A lack of major SSWs in the modeling study of Gillett et al. [2009] could be one possible explanation for this discrepancy.

Based on these results, a more comprehensive investigation of ZAOH effects covering different time periods (e.g., over both NH and SH winter for different years) is warranted. These will examine the relative importance of ozone-modified wave propagation versus wave damping in modulating the planetary wave drag and thus the zonal-mean circulation.

Acknowledgments. We thank John Albers helpful discussions during the preparation of this manuscript. JPM was supported in part by the Office of Naval Research and in part by the NASA Heliophysics Living With a Star Program award number NNH08AI67I. TRN was supported in part by NSF Grant ATM-0733698 and by NASA/NRL Grant NNH08AI67I. ECC was supported by NSF's Faculty Early Career Development (CAREER) Program, Grant ATM-0449996.

References

Charlton, A. J., et al. (2007), A new look at stratospheric sudden warmings. Part II: Evaluation of numerical model simulations, *J. Climate, 20,* 470–488, doi: 10.1175/JCLI3994.1.

Cordero, E. and P. M. d. F. Forster (2006), Stratospheric variability and trends in models used for the IPCC AR4., *Atmos. Chem and Phys. 6*, 5369–5380.

Crook, J. A., N. P. Gillett, and S. P. E. Keeley (2008), Sensitivity of Southern Hemisphere climate to zonal asymmetry in ozone, *Geophys. Res. Lett., 35*, L07806, doi:10.1029/2007GL032698.

Eckermann, S. D., K. W. Hoppel, L. Coy, J. P. McCormack, D. E. Siskind, K. Nielsen, A. Kochenash, M. H. Stevens, and C. R. Englert (2009), High-altitude data assimilation system experiments for the Northern Hemisphere summer mesosphere season of 2007, *J. Atmos. Sol. Terr. Phys., 71*, 531-551.

Gabriel, A., D. Peters, I. Kirchner, and H. F. Graf (2007), Effect of zonally asymmetric ozone on stratospheric temperature and planetary wave propagation, *Geophys. Res. Lett., 34*, L06807, doi:10.1029/2006GL028998.

Gillett, N. P., J. F. Scinocca, D. A. Plummer, and M. C. Reader (2009), Sensitivity of climate to dynamically consistent zonal asymmetries in ozone, *Geophys. Res. Lett., 36*, L10809, doi:10.1029/2009GL037246.

Hoppel, K. W., N. L. Baker, L. Coy, S. D. Eckermann, J. P. McCormack, G. Nedoluha, G. and D. E. Siskind (2008), Assimilation of stratospheric and mesospheric temperatures from MLS and SABER in a global NWP model, *Atmos. Chem. Phys., 8*, 6103-6116.

McCormack, J. P., S. D. Eckermann, D. E. Siskind, and T. J. McGee (2006), CHEM2D-OPP: A new linearized gas-phase ozone photochemistry parameterization for high-altitude NWP and climate models, *Atmos. Chem. Phys., 6*, 4943–4972.

McCormack, J. P., K. H. Hoppel, and D. S. Siskind (2008), Parameterization of middle atmospheric water vapor photochemistry for high-altitude NWP and data assimilation, *Atmos. Chem. Phys. Discuss., 8*, 13,999–14032.

McCormack, J. P., L. Coy, and K. W. Hoppel (2009), Evolution of the quasi 2day wave during January 2006, *J. Geophys. Res., 114*, D20115, doi:10.1029/2009JD012239.

Meehl, G. A., *et al.* (2007), Global Climate Projections, in *Climate Change 2007: The Physical Science Basis. Contribution of Working Group I to the Fourth Assessment Report of the Intergovernmental Panel on Climate Change*, Solomon, S. *et al.*, eds. Cambridge University Press, Cambridge, United Kingdom.

Nathan, T. R. and E. C. Cordero (2007), An ozone modified refractive index for vertically propagating planetary waves, *J. Geophys. Res., 112*, D02105, doi:10.1029/2006JD007357.

Perlwitz, J., S. Pawson, R. L. Fogt, J. E. Nielsen, and W. D. Neff (2008), Impact of stratospheric ozone hole recovery on Antarctic climate, *Geophys. Res. Lett., 35*, L08714, doi:10.1029/2008GL033317.

Son, S.-W., *et al.* (2008), The impact of stratospheric ozone recovery on the Southern Hemisphere westerly jet, *Science, 320*, 1486, doi:10.1126/science.1155939.

Waugh, D. W., L. Oman, P. A. Newman, R. S. Stolarski, S. Pawson, J. E. Nielsen, and J. Perlwitz (2009), Effect of zonal asymmetries in stratospheric ozone on simulated Southern Hemisphere climate trends, *Geophys. Res. Lett., 36*, L18701, doi:10.1029/2009GL040419.

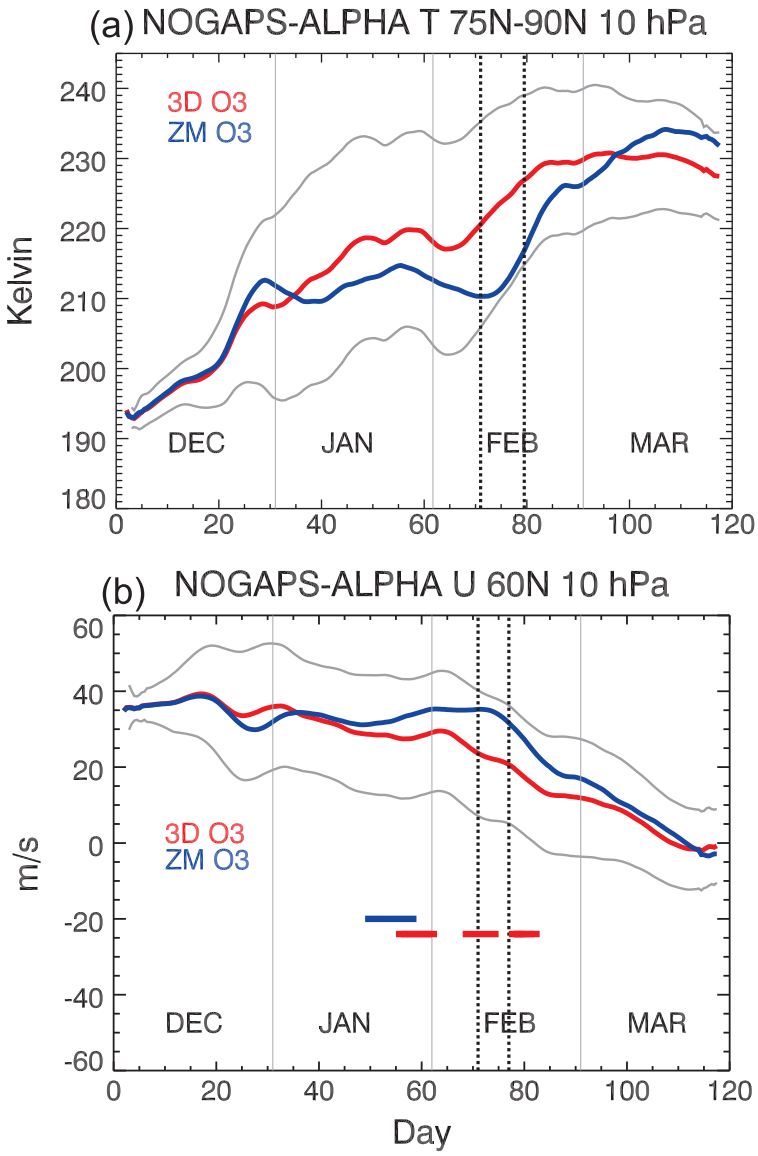

Figure 1. Time series of 3DO3 (red) and ZMO3 (blue) ensemble mean (a) temperatures and (b) zonal winds at 10 hPa beginning 1 December and ending 31 March. Temperatures are averaged over 75°N-90°N, zonal winds are for 60°N. Gray curves indicate the standard deviation computed from the 3DO3 ensemble members. Dotted vertical lines indicate when ensemble mean differences are statistically significant at the 95% confidence level based on Student's t-test. Red and blue horizontal lines in (b) indicate dates of stratospheric sudden warmings in the 3DO3 and ZMO3 ensembles, respectively.

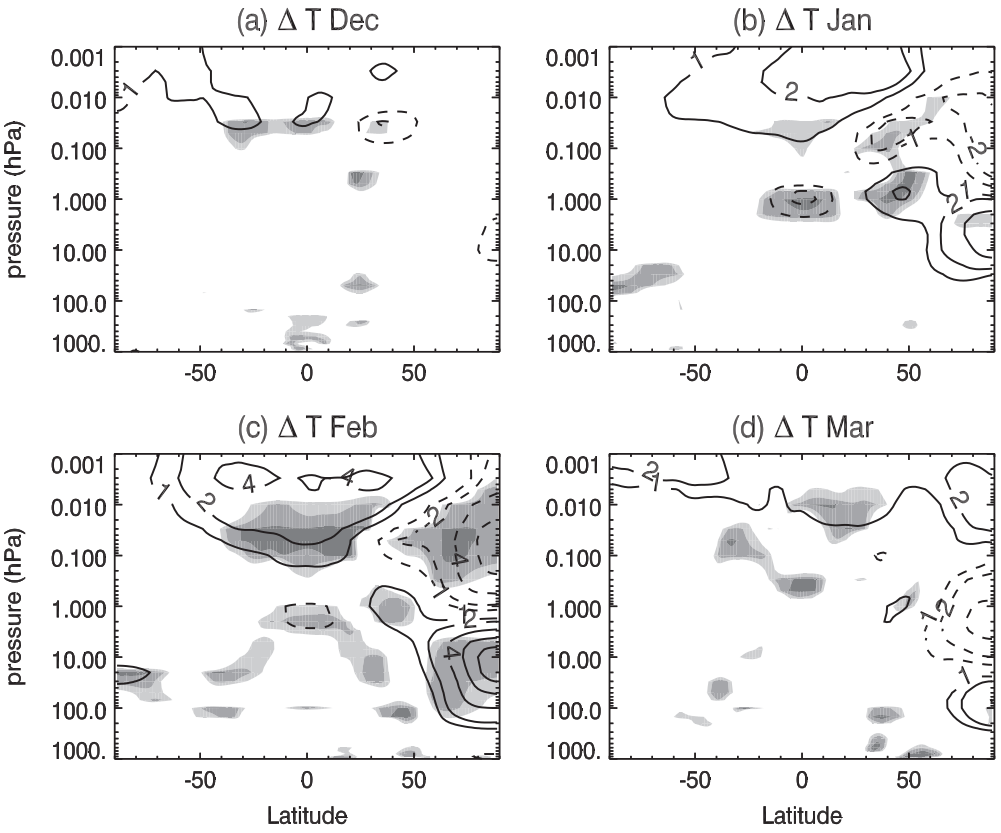

Figure 2. Monthly zonal mean temperature differences between the 3DO3 and ZMO3 ensembles (ΔT = 3DO3 minus ZMO3) for (a) December, (b) January, (c) February, and (d) March. Contours drawn at $\pm$1, $\pm$2, $\pm$4, $\pm$6, and $\pm$8 K. Solid (dashed) contours denote positive (negative) values. Shading indicates statistically significant differences at the 95% (light shading) and 99% (dark shading) confidence levels.

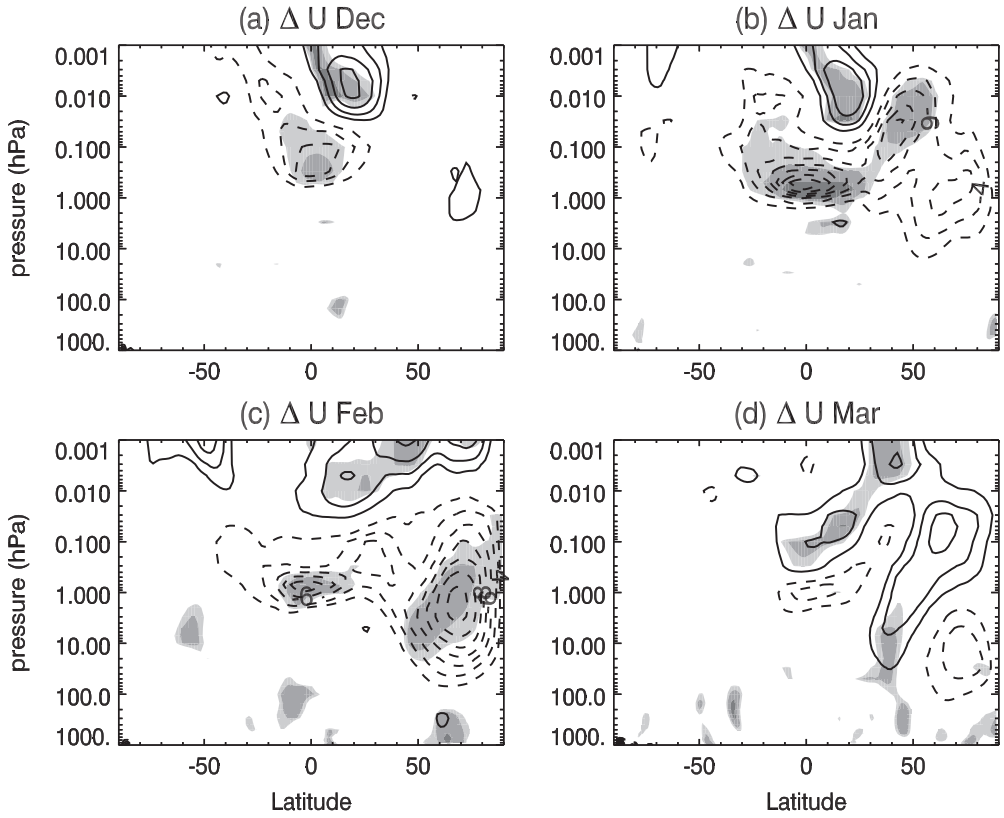

Figure 3. As in Figure 2, but for zonal mean zonal winds. Contour interval is ± 2 m s^{-1}, zero contour is suppressed.

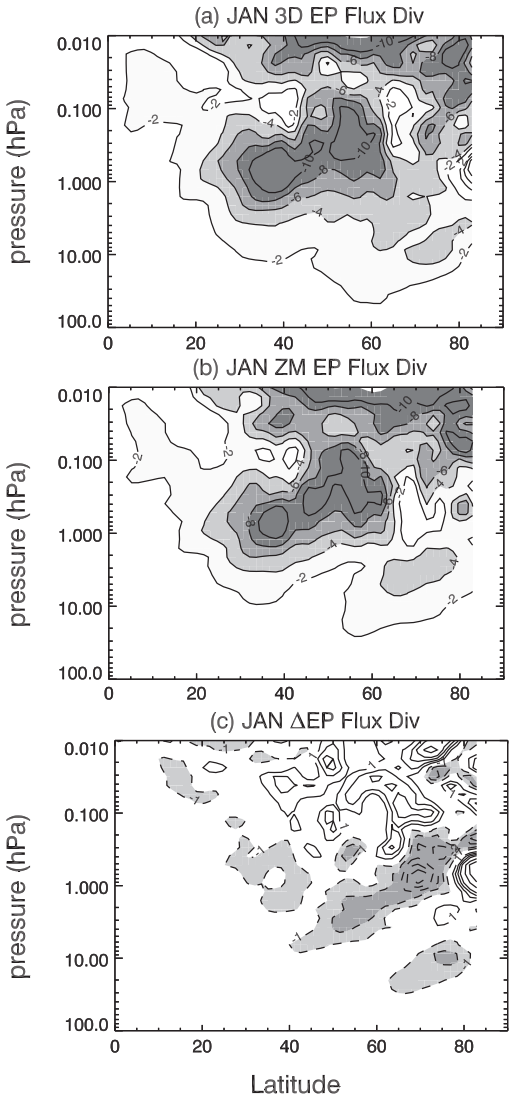

Figure 4. (a) 3DO3 ensemble mean EP flux divergence for January over the Northern Hemisphere. Contours drawn at -2, -4, -6, -8, and -10 m s^{-1} day^{-1}, values greater than 2 m s^{-1} day^{-1} are shaded; (b) ZMO3 ensemble mean EP flux divergence for January, as in (a); (c) difference plot of EP flux divergence (3DO3 minus ZMO3) for January, contours drawn every 1 m s^{-1} day^{-1}. Dashed contours denote negative values, and values less then 1 m s^{-1} day^{-1} are shaded.